Decompression profile and bubble formation after dives with surface decompression: Experimental support for a dual phase model of decompression.

A.O.BRUBAKK[1], A.J. ARNTZEN[2], B.R.WIENKE[3] and S.KOTENG[1]

[1]Department of Physiology and Biomedical Engineering, NTNU, N-7006 Trondhiem, Norway, [2]Barotech as, N-5000 Bergen, Norway, and [3] Computational Physics Division, Los Alamos National Laboratory, Los Alamos, NM 87545, USA.

Brubakk AO, Arntzen AJ, Wienke BR, Koteng S. Decompression profile and bubble formation after dives with surface decompression: Experimental support for a dual phase model of decompression. Undersea Hyperb Med 2003; 30(3): 181-193 - The present study was initiated in order to determine the effect of decompression profiles on bubble formation following surface decompression using oxygen. Following an air dive to 496 kPa (130 fsw) for 90 minutes, three different profiles were tested in the pig; a USN staged decompression profile, a profile using linear continuous decompression with the same total decompression time as the USN profile (ABI) and a linear profile with half the total decompression time compared to the the first two (ABII). The subsequent surface decompression at 220 kPa lasted 68 minutes for all three schedules. The study demonstrated that, following final decompression, the two linear profiles produced the lowest amount of vascular gas, with the fastest profile producing significantly less bubbles in the Pulmonary artery than the other two. Similar results were obtained in the jugular vein. The results are in qualitative agreement with model simulation using the Reduced Gradient Bubble Model (RGBM), demonstrating that the controlling tissues are reduced from those with a half time of 40 minutes using the USN procedure to 5 minutes using the fastest linear profile.

Pulmonary artery bubbles, jugular vein, Reduced Gradient Bubble Model, surface decompression.

INTRODUCTION

There is general agreement that decompression illness (DCI) is caused by the formation of a gas phase after decompression. To prevent this, many different decompression schedules have been proposed. Most decompression schedules used in commercial and recreational diving are based on the principles first described by Boycott et al 1908 (1). This model strives to set up a sufficiently large gradient for gas elimination and assumes that substantial supersaturation can be tolerated without significant bubble formation. A number of subsequent decompression models have been based on these principles. One feature of these models is that the number of tissue compartments have increased significantly over the years and the longest time constants for these compartments have increased from 75 minutes in the model of Boycott et al in 1905 to 1280 minutes in the model of Miller et al in 1970 (2).

Hills described an alternative model, where bubble formation would happen as soon as supersaturation was present, suggesting that bubble formation would occur early in the Haldanean type models and that long decompressions from severe dives would be needed to allow their elimination (3).

Surface decompression with oxygen (SuDO2) is used extensively in commercial diving. This procedure has the advantage that the time in water is reduced. The diver in the water is decompressed quickly and returned to a deck chamber breathing oxygen under pressure. This procedure gives similarly safe results as standard in-water decompressions and has the advantage that divers can spend the main part of the decompression in a dry environment (4).

Decompression procedures for deep and long air dives are not satisfactory. According to the data of Shields et al., these dives have a significantly higher incidence of decompression sickness than less stressful dives (5). Interestingly, there was no difference in performance of the many decompression tables, using both in-water and SurDO2 decompression, in use at that time. This led to the introduction of limitations in bottom time in the deeper range by the Health and Safety Executive in the UK (HSE).

Recently, there have been several air diving operations in Norway with unacceptably high incidences of DCI in dives using SurDO2 deeper than 30 msw (Arntzen Personal communication). The air tables used in Norway are derived from the commonly used US Navy tables with extensions to make them more conservative. This animal study was designed to see if differences in air decompression profile in the in-water phase would influence bubble production following surface decompression using oxygen.

MATERIALS and METHODS

Sixteen pigs of both sexes, aged 10-11 weeks, mean weight 22.6 kg (range 20- 24 kg), were used in this study. The animal experiments were conducted in conformity with "Principles of Laboratory Animal Care" (NIH Publication No 85-23, revised 1985). The experimental protocol was reviewed and approved by the Norwegian Council for Animal Experiments.

The pigs were fasted for 40 hours with free access to water. Thirty minutes before induction of anesthesia, the pigs received premedication: 7-9 mg/kg azperonum (Sedaprone®, Janssen) was given intravenously. Atropine sulfate (1 mg Atropin, Hydro Pharma) was given intravenously via an ear vein and anesthesia was induced by thiopental sodium (5 mg/kg, Thiopenton Natrium, Nycomed Pharma) and ketamine (20 ml/kg, Ketalar, Parke Davis). Anesthesia was maintained throughout the experiment by continuous infusion of ketamine in 0.9% NaCl (10-15 mg $\cdot$ kg^{-1} h^{-1}) and bolus doses of α-chloralose in 0.9% NaCl (10-15 mg $\cdot$ kg^{-1}, 0.25% solution). A tracheostomy tube was placed and the animals breathed spontaneously in the supine position. Depth of anesthesia was maintained by observation and measurements of arterial CO_2 and O_2 tensions, respiratory frequency and heart rate. During hyperbaric exposures, anesthesia was maintained through a remotely controlled infusion pump inside the chamber. During surgery, body temperature was monitored by a rectal probe and maintained at 38^{o}C using a heating pad. The temperature inside the chamber was automatically regulated to maintain a stable body temperature of 38 $\pm$ 0.3^{o}C. Arterial and venous blood samples were taken at regular intervals from ear arteries and veins during the exposure and analyzed for pCO_2 and pO_2 using an ABL 330 Blood Gas Analyzer (Acid-Base Laboratory, Radiometer, Copenhagen). The blood gases were corrected for changes in rectal temperature using standard methods.

A 5.0 MHz transesophageal ultrasonic transducer was introduced into the mouth and advanced to a position about 30 cm into the esophagus where a clear view of the pulmonary artery, the right ventricle and the aorta could be seen. The transducer was connected to a CFM 750 ultrasonic scanner (Vingmed Sound a/s, Horten, Norway). The data was transmitted to a computer where the number of bubbles were continuously monitored using a specially developed program (6). The number of bubbles in the pulmonary artery is given as bubbles / cm^2.

An ultrasonic Doppler instrument was used to detect gas bubbles in the right or left jugular vein in Group 2 and 3 (Alfred, Vingmed Sound A/S, Horten, Norway). Due to technical problems, these recordings were not performed in Group 1. 10 MHz ultrasonic transducers were placed around the vessels. The amplitude of the reflected signal was recorded continuously. During the stabilizing period, the reflected amplitude from the flowing blood was determined. An increase in ultrasonic amplitude following the dive was considered to be caused by gas bubbles and the amplitude proportional to the volume of gas in bubbles. We have demonstrated that the reflected ultrasonic intensity is independent of blood flow and hematocrit (7).

Pulmonary artery bubble counts and ultrasonic amplitude values were time averaged using a 5 point moving function. The PA bubble counts were sampled each minute throughout the experiment. The peripheral amplitude readings were sampled each minute except during the interval of 20 minutes before and after reaching normobaric pressure, when they were sampled each 15 seconds.

The model:

A number of phase separation models have been developed over the years that describe bubble formation and allow simulation of the effect of bubbles on gas kinetics. We used a dual phase model, called the Reduced Gradient Bubble Model (RGBM) (8-10), that tracks both dissolved gas build-up and free phase (bubble) growth during and after compression-decompression. The model has been fitted to diving data and forms the basis for recent mixed gas diving tables and commercial technical diving software (10,11). The model (RGBM) recovers standard Haldane behavior for short and shallow exposures, but extends dissolved and free phase dynamics for deep, decompression, repetitive, and mixed gas exposures. Unlike the Varying Permeability Model (12,13) the RGBM uses realistic equations of state (EOS) to describe the behavior of bubble skins (surfactants) under pressure changes, as well as film structure diffusivity to gas transfer (11), tracks expansion and contraction under pressure changes, and assigns persistence time scales based on surfactant structures. Details of the model can be found in (11) and at *www.RGBMdiving.com*, and only the principles will be given here.

The model assumptions are fairly simple. From any distribution of seed nuclei excited into growth by compression-decompression, a certain critical radius, ε, separates growing from contracting seed nuclei. Over time, a separated phase integral constraint is satisfied for decompression, and a temporal phase function is tracking bubble excitation, gas diffusion across bubble interfaces, and Boyle expansion-contraction of mass transport coefficient (diffusivity times solubility). Integrals in the temporal expressions run from ε, the excitation radius, out to some convenient (large) cutoff, summing up separated phase following excitation, gas diffusion, and Boyle expansion-contraction.

Sets of arbitrary tissues are assigned (3 minutes to 640 minutes halftimes), and the integral is computed across all tissues for any exposure and all time. All parameters in the RGBM (some 8 - 10), except equations of state, have been fitted to data in maximum likelihood,

yielding a robust computational model. The tissue equations are the usual exponential expressions for the instantaneous gas tensions.

The computational flow is as follows. First, maximum supersaturation is estimated across all seed radii for a given surface tension and dissolved gas tension. This is used to stage the diver to the surface. Separated phase volume is then computed at the surface for the whole process. The process is iterated (phase integral) to closure in time, at steps of 10 fsw in the ascent., across all tissue compartments, by reducing the supersaturation gradient until the separated surface phase is less than a fitted limit for decompression staging.

Experimental procedures:

All animals were compressed to 496 kPa (130 fsw) at a rate of 100 kPa /minute. They were kept at depth for 90 minutes. The animals were divided into three groups and decompressed breathing air using different decompression procedures.

Group 1	N= 7	USN
Group 2	N= 6	ABI
Group 3	N= 3 (6)	ABII

Animals in group 1 and 2 were exposed once, and animals in group 3 were exposed twice four days apart. In a pilot study we have shown no difference in bubble formation between exposures four days apart (unpublished).

The three tested decompression schedules are shown in Figure 1 and Table 1. Schedule ABI was chosen to be of the same length in time as the USN schedule, but with a slower ascent speed. In ABII decompression speed was increased by 50% relative to ABI and the stop at 190 kPa (30 feet) was reduced by 50%, thus giving a total decompression time 50% less than that of ABI. Following decompression to the surface, the animals were kept there for 3 minutes and then recompressed to 220 kPa (40 fsw) in 0.5 minutes breathing oxygen. Oxygen breathing continued for 68 minutes, after which the animals were decompressed to the surface in 2 minutes. The animals were observed for 120 minutes breathing air and then killed with intravenous KCl while still under anesthesia.

Figure 1. In-water decompression profiles.

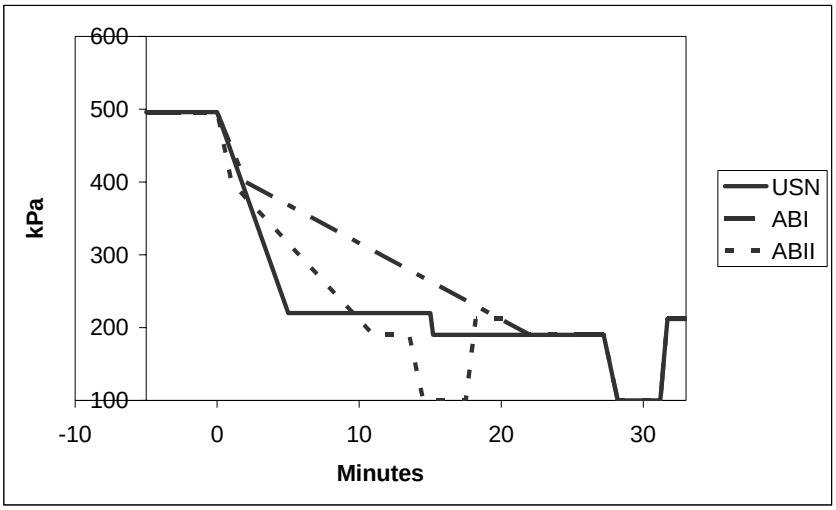

Table 1. Decompression schedules.

		Stop at		Total Dec.time
		220 kPa (40 fsw)	190 kPa (30 fsw)	
USN	Staged decompression Ascent speed 100 kPa /min	10 min	14 min	28 min
ABI	Linear decompression * 10 kPa / min.	NA	5 min	28 min
ABII	Linear decompression * 20 kPa / min.	NA	2.5 min	14 min

* 496 – 390 kPa was decompressed in two minutes in ABI and in one minute in ABII

Statistics:

The maximum values of the bubble counts and the amplitudes in each group were compared using the Mann-Whitney U-test. After final surfacing the mean values of the bubble counts and amplitudes were compared for the ten minutes starting 5 minutes after reaching surface. $P<0.05$ was set as level of significance.

RESULTS

Bubbles appeared immediately prior to surfacing or during the surface interval. There was no difference in bubble production between the second and first dive performed by the animals in group 3, and they were therefore treated as independent dives. There was no difference in bubble production at the end of the surface period between USN and ABI, but the number of bubbles for ABII was significantly less. Immediately on reaching 220 kPa following recompression, there was considerable variation in bubble numbers in all groups, with no significant differences between them. However, four minutes after reaching 220 kPa there was a significant difference between schedules, and at the end of the stay at 220 kPa, no bubbles were seen for the AB schedules. Immediately after return to surface, there was considerable variability in the number of bubbles, in particular on the two AB schedules (group 2 and 3) where the number of bubbles was very low. Thus, in order to avoid these apparently random variations, the average of the maximum bubble numbers were determined for a period of ten minutes starting 5 minutes after reaching surface, which was considered a reasonable time for stabilization. In this ten minute period, there were significantly fewer bubbles on the two AB schedules then on the USN schedule and the ABII schedule produced significantly fewer bubbles than the ABI. The results can be seen in Table 2 and Figure 2.

Table 2. Pulmonary artery bubbles

Schedule	Max AP SI	Max220 kPa	MaxER	Max Surface
		bubbles / cm^2		
USN	1.8±0.9	1.4±1,2	0.1±0.1	1.2±1.1
ABI	1.7±1.7	0.2±0.2*	0*	0.06±0.01*
ABII	0.04±0.04*	0.03±0.005*	0	0.002±0.002*

Max AP SI = maximum bubble numbers at end of surface interval; Max 220 kPa = maximum bubble numbers four minutes after recompression; MaxER = maximum bubble numbers at end of recompression at 220kPa after 68 minutes breathing O_2. Max Surface = average of maximum bubble numbers for ten minutes at surface after 68 minutes O_2 breathing at 220 kPa. * = significantly different from USN or ABI profile.

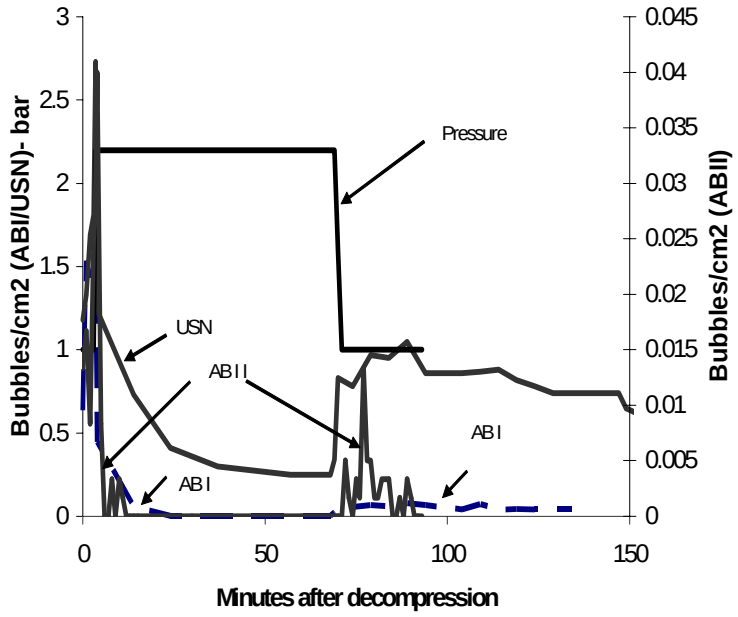

Figure 2. Bubbles in the Pulmonary Artery; note y-axis for ABII is to the right. The pressure is given in bar on the left axis in order to display the results in one graph, 1bar = 100 kPa.

Bubbles in the jugular vein were recorded for the two AB schedules. As can be seen from Figure 3**,** there is an apparent difference between the two schedules. At the end of the surface interval, the amplitude of the reflected signal is 56.1 ± 51.4 and 22.3 ± 18.3 (AU) on the ABI and ABII profile respectively, while at surface after recompression the values were 1.44 ± 4.1 and 0.35 ± 1.5 (AU) respectively. These differences are however not significant.

Simulations:

Calculations were performed for the three profiles (USN, ABI, and ABII) using the above sets of equations and production code DECOMP (14). The code permits calculation of Haldane or RGBM staging procedures for arbitrary gas mixtures with fixed separated gas phase Φ or calculation of Φ for a given profile and staging model (Haldane or RGBM). The latter option was employed here for the three profiles. Results are summarized in Table 3 in terms of separated phase and controlling tissue at the surface. Calculations of separated phase are normalized to 1.000 for the USN profile at the surface interval. As can be seen, the simulations show the same relative ranking of the profiles as the experimental results.

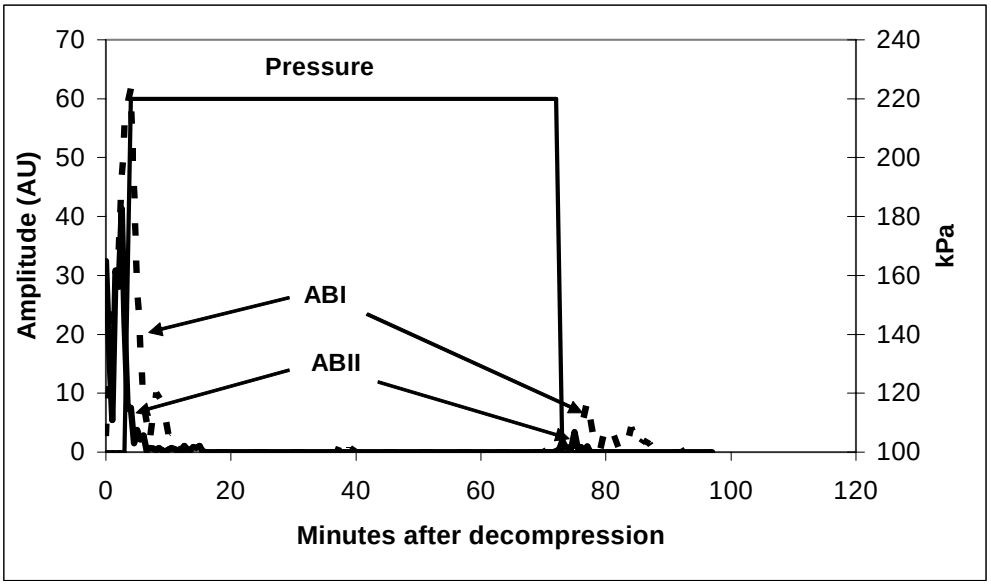

Figure 3. Bubbles in the jugular vein. The amplitudes are given in Arbitrary Units relative to the amplitude of the flow signal. The pressure of recompression is given in msw in order to display the profile on the same graph as the results, 10 msw = 100 kPa.

Table 3. Simulations of the three profiles.

	USN	ABI	ABII
Φ (separated phase), relative volume			
*	1.000	0.478	0.0255
**	0.630	0.120	0.004
τ (controlling tissue), minutes			
*	60.0	20.0	10.0
**	40.0	10.0	5.0

* At the end of the surface interval before recompression. ** At surface after 68 minutes of oxygen breathing at 220 kPa. Note: The separated volume of gas is set equal to one for the USN profile in the surface interval; all other values are relative to this.

In Table 4, a comparison between the simulations and the experimental results has been made, assuming that the number of bubbles in the pulmonary artery is proportional to the volume of gas in bubbles (see Discussion). As can be seen, the results are in close agreement for the USN profile, but the simulations largely underestimate the reduction in gas volume observed in ABI and ABII.

Table 4. Comparison of changes in gas phase volume between profiles: Model vs. observations in %, values for USN at end of surface interval is set at 100%.

	USN		ABI		ABII	
	Model	Observe	Model	Observe	Model	Observe
End of surface interval	100	100	48	94	2.6	2
At surface after oxygen breathing.	63	70	12	1,7	0.4	0.1

DISCUSSION

This study has demonstrated that the procedure used for decompression to the surface will have a significant effect on the number of bubbles formed in the venous system both during the surface interval and after oxygen breathing in the chamber. Moving from staged to a linear profile of similar duration significantly reduced the number of bubbles at the end of decompression. A further increase of 50% in ascent rate of the linear profile eliminated nearly all gas in the pulmonary artery. At the end of decompression, ABI produced about 5% less bubbles than the USN profile, while the ABII procedure reduced this amount to 3% of the ABI.

The change in profile also led to a significantly faster reduction in the number of bubbles after recompression to 220 kPa. While the two AB profiles eliminated all bubbles from the pulmonary artery during oxygen breathing, gas could still be detected at the end of the 68 minute period at 220 kPa on the USN profile. The reduction in bubble formation was also reflected in the jugular vein, where the ultrasonic amplitudes were lower on the ABII profile (Figure 3**)**. None of these differences were significant, probably due to very large standard deviations.

It is reasonable to assume that the amount of gas taken up during the bottom phase is similar in all animals. Previous studies have shown that a 90 minute exposure will lead to a 98% saturation of nitrogen of the venous blood in pigs (15). Thus we consider the differences seen as being a result of the difference in decompression procedures.

The decompression rate used in ABI is significantly slower than that used by the USN procedure. Reducing decompression rate while maintaining a short decompression stop at a shallow depth (in this case 190 kPa, 30 feet) is well in agreement with current recommendations for safe diving given by a number of diving organizations (PADI, NAUI, CMAS) However, it is

generally accepted that the decompression rate used for the USN table (100kPa / minute) is slow enough to prevent significant bubble formation. This study has demonstrated that a slower ascent rate significantly reduces bubble formation compared to a faster rate and a longer decompression stop. Although there was no significant difference in the number of bubbles seen at the end of the surface interval, it is noteworthy that the rate of elimination of bubbles after recompression was significantly faster on the ABI profile and that no bubbles could be seen at the end of recompression on this profile. Recompression to 220 kPa will reduce the volume of the gas bubbles by approximately 50%. That the bubbles disappear much faster could mean that the bubbles are smaller on the ABI profile and the fact that only few of them re-appear after surfacing would indicate that less inert gas is present. Probably the most surprising finding was that by increasing the decompression rate (ABII compared to ABI), although still slower than that used by the USN procedure, far less gas was produced (see below).

The USN diving tables have been developed using a Haldanean model, where decompression is determined by the kinetics of gas elimination. According to this model, all gas is in solution and the different tissues can tolerate a certain supersaturation before DCI will occur. By inference, in these models it is also assumed that no bubbles will form before these supersaturation levels are reached.

Using a dissolved gas model, it is reasonable to perform a rapid decompression to a tolerable lower pressure to set up a gradient that will assist in eliminating the excess inert gas. However, there is evidence from many studies that gas bubbles occur in the venous system during most decompressions using this type of procedure (16-19). Data of Eckenhoff et al (20) indicate that once the sum of the partial pressures of all gases exceeds the environmental pressure, gas formation occurs in the venous system. The predominant theory about the growth of bubbles is that they grow from pre-formed nuclei; the energy required to generate a bubble "de novo" is considerable and high levels of supersaturation are needed to develop a gas phase in "pure solutions" (21). These nuclei may be composed of small (approx. 1 micron diameter) stable gas bubbles (22).

One important effect of bubble formation is its effect on the dynamics of gas elimination. When gas bubbles form and expand they may obstruct the arterial and venous circulation, leading to tissue ischemia, or they can damage the tissue and induce pain by direct pressure effects. Bubble formation may influence circulation by mechanical obstruction. Venous obstruction may lead to edema and arterial obstruction may lead to tissue ischemia, both of which have been observed after decompression (23). This can reduce gas elimination by increasing diffusion distances and by reducing blood flow.

Both theoretical (24) and experimental (25) studies have demonstrated that gas bubbles in the tissue will increase gas elimination time. This is partly taken into account by the new US Navy diving tables, where gas elimination is considered to be linear, not exponential (26). However, in reality the problem may be even more complex as bubbles in the circulation may increase the transport of gas to the lungs (27). The results presented here indicate that bubble formation may indeed reduce elimination rate of inert gas.

In the pulmonary artery, the number of gas bubbles was counted continuously.
We have shown that this count is linearly related to the amplitude of the Doppler signal in a peripheral vein (28), indicating that the bubble number is proportional to the volume of gas (see below). The intensity of the reflected ultrasonic signal from a gas bubble is proportional to the scattering cross-section which for bubbles above resonant size is similar to the geometric cross-section, while the amplitude is proportional to the square root of this cross-section (29). The

bubble radius for resonance is in the order of 0.3 μm at 10 MHz; gas bubbles following decompression will probably have a size considerably above this. For the bubble concentrations likely to be seen in the vessels, the reflected intensity from all bubbles can simply be added up (30).). In the jugular vein, the amplitude of the reflected signal was recorded continuously. During the stabilizing period, the amplitude from the flowing blood was determined. An increase in amplitude following the dive was considered to be caused by gas bubbles. We have demonstrated that the reflected ultrasonic intensity is independent of blood flow and hematocrit (7). The values given in this paper are amplitudes above the background signal. A previous study demonstrated that there was a proportional increase in Doppler amplitude with increasing bubble numbers (28), indicating that the bubbles all are of a similar size and thus the volume of gas in the vessel will be proportional to the increase in amplitude above the background signal..

Based on the assumptions above, changing the decompression profile from USN to ABI reduced the separated gas volume in the total venous drainage by 95 %. A further reduction of 99.7 % occurred when the ABII was used, this procedure led to a reduction of 99% of separated gas in the venous drainage from the brain when compared to ABI. The differences are probably even larger than this, as the bubbles seen at the surface interval after the USN were probably larger than those observed after ABI, as the latter disappeared significantly faster at 220 kPa.

It is probably not surprising that a slower decompression rate will reduce bubble formation. This is what was seen when ABI was used instead of the USN profile. It is however counterintuitive that a doubling in decompression speed (ABII compared to ABI) and a reduction of the decompression stop will have such a dramatic effect on gas bubble formation, as the calculated gas volume of the ABII profile at the end of the procedure was only 0.3% of that seen after ABI (Table 2). In order to try to understand this, it was decided to perform a simulation using a model. The model chosen was the RGBM described above. The simulations show that the model accurately describes the ranking between the different three profiles.

The similarity in the results obtained from the experiments and the simulations support the value of this model approach. Keeping in mind that the above are comparative model estimates, a few comments are fairly obvious regarding the phase dynamics and differences between USN and ABI, ABII (as seen at the surface):

1) Profiles ABI and ABII result in smaller amount of separated gas, compared to USN.

2) Faster compartments control ascents for ABI and ABII.

3) Computed separated phase is still large for USN even after pure oxygen at 220 kPa for 68 minutes, while very much smaller for ABI and ABII .

These trends are characteristic of phase models versus dissolved gas models. The choice of the particular model used was determined by the fact that this model is well documented and has been extensively used in a number of tables and dive computers.

It is important to note, however, that the comparison between the observed data and the output from the model (Table 3) shows that the model significantly underestimates the reduction in gas phase achieved by changing the decompression profile following the completion of oxygen breathing. This is particularly apparent for the ABII profile. The reason for this discrepancy is not clear, but may be a result of using a model of bubble formation calibrated by using the incidence of decompression sickness to predict bubble formation in the pulmonary

artery. It may also indicate that faster tissues play a much more significant role in bubble formation than is assumed in this model and that other gas separation models may give a better fit to the data.

The model simulations show that at the surface following the full procedure, the time constants of the controlling tissue changes from 40 to 5 minutes. Using Haldane type models, the longer the exposures, the more the tissues with long time constants dominate. However, the experimental basis for this has come from exposures using decompressions that probably produce a significant number of gas bubbles which in turn will significantly increase elimination time for gas (24). The results presented in this study indicate that even at long exposures, fast tissues dominate and the apparent influence of slow tissues may be an experimental artifact caused by bubble formation.

It has been suggested that there is little relationship between gas bubbles detected in the pulmonary artery and clinical signs of decompression illness (DCI). The main reason for this is that gas bubbles have been detected in the absence of symptoms (17). However, the statistical risk of DCI increases with increasing number of bubbles. Several studies have documented the relationship between the occurrence of many venous bubbles and the risk for clinical symptoms requiring treatment (16,17,31,32). In our experience, having monitored many hundreds of air dives and numerous saturation dives, clinical symptoms do not occur in the absence of pulmonary artery gas bubbles. Nishi (17) points out that for air dives, decompression illness was always accompanied by vascular bubbles. Sawatzky (33) has shown that there is a 5-10% risk of decompression illness in individuals with a single observation of grade III - IV bubbles, using the grading system developed by Spencer et al (31,34). In this study, changing from the USN to the ABI profile reduced the Spencer Grade from III to I, using the conversion scale previously published (28, 35). As indicated by the results of applying procedure ABII, aiming for bubble free decompression is possibly both a useful and attainable goal (36).

The relevance of animal experiments to human diving procedures can always be argued. Obviously, caution must be used when extrapolating these results to divers working in the water. The present study was performed in anesthetized young pigs. However, we maintain that the experimental model can be used to give relative risk of the different procedures. A previous study from this laboratory showed that, following decompression from saturation dives, this animal model, using pulmonary artery gas bubbles as the end point, gave results that were compatible with what was seen in man using decompression sickness as the endpoint (37). In that study, different ascent speeds and oxygen tensions were used, accurately ranking the different procedures.

In the present study, the standard USN decompression profile was compared to experimental profiles of the same total duration or shorter, but with a different in-water profile. The profiles used (AB) were not based on a mathematical model, but were designed to test if decompression following a slower in-water profile would give less gas bubble production. In addition, the profile was designed for ease of use in practical operations. At the end of the observation period, the number of gas bubbles in the pulmonary artery was similar to Grade I-II on the Spencer scale in the two AB groups, while it was Grade III in the USN group (35).

The results presented here indicate that phase models more accurately describe the decompression process and this may have impact on the development of decompression schedules for diving, bearing in mind that these results must be verified in further studies. There are several ways to improve decompression procedures using surface decompression. It is reasonable to assume that an increase in oxygen content in the breathing gas during

decompression as well as an extension of the time breathing oxygen at 220 kPa would reduce the amount of separated gas phase after the dive. The procedure described in the present study would seem to have a considerable advantage.

ACKNOWLEDGEMENTS

The assistance of Anne-Lise Ustad in performing the experiments and Astrid Hjelde for statistical help is appreciated. The contribution of Valerie Flook to the initial part of this study is gratefully acknowledged. This study was in part financed by grants from The Norwegian Employers Association (NHO) and Statoil, Hydro and Esso as part of their research and development program in diving.

REFERENCES

1. Boycott, AE., Damant, CC., and Haldane, JS. The Prevention of Compressed - Air Illness. J Hyg, London 1908;8:342-443.
2. Berghage TE., Goehring, GS., and Donelson C. Pressure Reduction Limits for Rats Subjected to Various Time/Pressure Exposures. Undersea Biomedical Research. 1978;5(4):323-34.
3. Hills, BA. Vital Issues in Computing Decompression Schedules From Fundamentals. I. Critical Supersaturation Versus Phrase Equilibration. Int J Biometeror 1970;14(2):111-28.
4. Imbert, JP.; Bontoux, M. Diving data bank: A unique tool for diving procedures development1988Houston, Texas: 20th Annual OTC; 1988.
5. Shields, TG, Duff, PM, Lee, WB, and Wilcock, SE. Decompression sickness from commercial offshore air-diving operations on the UK continental shelf during 1982 to 1986. Aberdeen: Robert Gordon's institute of technology; 1989. Report No.: OT 0 - 89 - 029.
6. Eftedal, O and Brubakk, AO. Detecting Intravascular Gas Bubbles in Ultrasonic Images. Med.& Biol.Eng.& Comput. 1993;31:627-33.
7. Brubakk, AO.; Torp, H. Ultrasonic methods for monitoring decompression. Nashimoto, I. and Lanphier, EH. Decompression in surfaced-based diving. Bethesda,MD.: Undersea and Hyperbaric Medical Society Inc; 1987. pp.107-14.
8. Wienke, B. R. Reduced Gradient Bubble Model. .Int.J.Biomed.Comput. 1990;26:237-56.
9. Wienke BR. Numerical Phase Algorithm for Decompression Computers and Applications. Comp Biol Med 1992;22:389-406.
10. Wienke BR. Bubble Number Saturation Curve and Asymptotics of Hypobaric and Hyperbaric Exposures. Int J Biomed Comp 1991;29:215-25.
11. Wienke BR., Technical diving in depth. Flagstaff: Best Publishing Company; 2001.
12. Yount DE. Skins of Varying Permeability: A Stabilization Mechanism for Gas Cavitation Nuclei. J.Acoust.Soc.Am. 1979;65(6):1429-39.
13. Yount DE. and Strauss RH. On the Evolution, Generation and Regeneration of Gas Cavitation Nuclei. J Acoust Soc Am 1982;65:1431-9.
14. Wienke BR. DECOMP: Computional Package for Transport Modeling in Tissues. Comp Phys Comm 1986;40:327-36.
15. Flook, V, Holmen, IM, Koteng, Ø, Koteng, S, Ustad, A-L, Eftedal, O, and Brubakk, AO. The effect of bottom time on inert gas washout and decompression bubbles in pigs. Trondheim, Norway: SINTEF; 1993. Report No.: STF23 F93024. (HADES project;vol.
16. Nishi RY. Doppler and ultrasonic bubble detection. Bennett, PB. and Elliott, DH. The physiology and medicine of diving. 4th ed. London: WB Saunders Company; 1993. pp.433-53.
17. Nishi RY. Doppler evaluation of decompression tables. Lin, YC. and Shida, KK. Man in the sea. San Pedre: Best Publishing Company; 1990. pp.297-316.
18. Spencer, MP. Decompression Limits for Compressed Air Determined by Ultrasonically Detected Blood Bubbles. J Appl Physiol 1976;40:229-35.

19. Gardette B. Correlation Between Decompression Sickness and Circulating Bubbles in 232 Divers. Undersea Biomed Res 1979;6(1):99-107.
20. Eckenhoff, RG., Olstad, CS., and Carrod, G. Human Dose-Response Relationship for Decompression and Endogenous Bubble Formation. J Appl Physiol 1990;69(3):914-8.
21. Hemmingsen EA. Nucleation of bubbles in vitro and in vivo. Brubakk, AO., Kanwisher, J., and Sundnes, G. Diving in animals and man. Trondheim: Tapir Publishers; 1986. pp.43-59.
22. Yount DE. Growth of bubbles from nuclei. Brubakk, AO., Kanwisher, J., and Sundnes, G. Diving in animals and man. Trondheim: Tapir Publishers; 1986. pp.131-64.
23. Francis TJR.; Gorman DF. Pathogenesis of the decompression disorders. Elliot, DH. and Bennett PB. The Physiology and Medicine of Diving. 4 ed. London: WB Saunders; 1993. pp.454-80.
24. Van Liew HD. and Burkard ME. Density of Decompression Bubbles and Competition for Gas Among Bubbles, Tissue, and Blood. J.Appl.Physiol. 1993;75(5):2293-301.
25. D'Aoust BG., Smith, K. H., and Swanson, H. T. Decompression-Induced Decrease in Nitrogen Elimination Rate in Awake Dogs. J.Appl.Physiol. 1976;41(3):348-55.
26. Thalmann ED., Parker EC, Survanshi, S., and Weathersby PK. Improved Probabilistic Decompression Model Risk Predictions Using Linear- Exponential Kinetics. Undersea & Hyperbaric Med 1997;24(4):255-74.
27. Kindwall, EP., Baz, A., Lightfoot, E. N., Lanphier, E. H., and Seireg, A. Nitrogen Elimination in Man During Decompression. Undersea Biomed.Res. 1975;2(4):285-97.
28. Brubakk AO.; Eftedal, O. Evaluation of reverse dive profiles. Lang MA and Lehner CE. Reverse Dive Profiles. Washington: Smithsonian Institution; 2000. pp.111-21.
29. Medwin, H. Counting Bubbles Acoustically:a Review. Ultrasonics 1977;15:7-13.
30. Angelsen, BAJ. A Theoretical Study of the Scattering of Ultrasound From Blood. IEEE Transactions on Biomedical Engineering 1980;BME-27(2):61-7.
31. Spencer MP. and Johanson, DC. Investigation of new principles for human decompression schedules using the Doppler ultrasonic blood bubble detector. Seattle: Tech Report, Inst Environ Med and Physiol; 1974.
32. Nashimoto I.; Gotoh Y. Relationship between precordial Doppler ultrasound records and decompression sickness. Schilling CW. and Beckett MW. Underwater Physiology VI. Bethesda: Undersea Medical Society; 1978. pp.497-501.
33. Sawatzky, KD. The relationship between intravascular Doppler-detected gas bubbles and decompression sickness after bounce diving in humans. York University, Toronto; 1991.
34. Smith KH. and Spencer, MP. Doppler Indices of Decompression Sickness: Their Evaluation and Use. Aerospace Medicine 1970;41(12):1396-400.
35. Eftedal, O; Brubakk AO.; Nishi RY. Ultrasonic evaluation of decompression: The relationship between bubble grades and bubble numbers. Undersea & Hyperbaric Med 25[Suppl], 35-36. 1998..
36. Flook V and Brubakk AO. Designing Bubble Free Decompression Profiles - Impossible ? Underwater Technology 1993;19:23-9.
37. Reinertsen, R. E., Flook, V., Koteng, S., and Brubakk, A. O. Effect of Oxygen Tension and Rate of Pressure Reduction During Decompression on Central Gas Bubbles. J.Appl.Physiol. 1998;84(1):351-6.

.